American Mineralogist, Volume 79, pages 205–214, 1994

Structure and bonding of calcite: A theoretical study

ANDREW J. SKINNER,* JOHN P. LAFEMINA
Molecular Science Research Center, Pacific Northwest Laboratory, P.O. Box 999, Richland, Washington 99352, U.S.A.
HENRI J. F. JANSEN
Physics Department, Oregon State University, Corvallis, Oregon 97331, U.S.A.

ABSTRACT

The ground-state structural and electronic properties of bulk calcite ($CaCO_3$) are calculated from first principles by working within the full-potential linearized augmented plane wave implementation of density functional theory. Calculated charge density plots for bulk calcite show clearly the mixed ionic and covalent bonding in this mineral. From these plots the relative size of the constituent atoms are determined by calculating bonded radii. In calcite, the O atoms are shown to be smaller than expected from ionic measures of the atomic size and of a similar size to the Ca atoms. Examination of the one-electron eigenfunctions and the computed density of states reveals the character of local bonding. Comparison of the computed density of states with recent X-ray photoemission data allows the orbital character of the experimental valence band peaks to be assigned. The highest occupied states are of O 2p character, with Ca 3p states mixing slightly with carbonate group states in the valence region. The calculated value of the band gap in calcite is consistent with the experimental value, as measured by reflection electron energy-loss spectroscopy. Lattice parameters are reproduced to within 5% of their experimental equilibrium values. Under pressure the carbonate group is shown to act as a rigid structural unit, with the C-O bond length decreasing by approximately 3 mÅ, for a 5% compression in volume.

INTRODUCTION

Calcite (rhombohedral calcium carbonate) is an environmentally important mineral. It acts as a buffer in sea water (Winchester, 1972), forms the major inorganic part of sea shells, and is secreted by some organisms, such as corals, to form solid skeletal structures (Schmalz, 1972). As a common component of soil, waste sludge, and ground water, it mediates the subsurface transport of heavy metal contaminants (Davis et al., 1987). Transparent calcite (e.g., Iceland spar), with its large birefringence, is important technologically, having applications in polarized optical devices (Hirano et al., 1991).

Our interest in calcite is in understanding its role in the transport of heavy metal contaminants. A microscopic knowledge of the bulk and surface chemistry of calcite and other carbonate minerals is critical to many groundwater contamination issues (Davis et al., 1987) and is important to the long-term cleanup of nuclear and chemical waste sites (Hochella and White, 1990). Although divalent metal cations are known to adsorb selectively on calcite in solution (Zachara et al., 1991), the process by which this happens on an atomic scale is not well understood (Hochella and White, 1990; Baer et al., 1991). Does this adsorption occur through direct cation substitution or through complex formation at the interface between ground water and calcite? What role does the electronic character of the constituent atoms play in this process? To interpret experimental results, a detailed knowledge of the electronic structure, local bonding, and relative size of the atoms in calcite is needed. This information is also critical in developing semiempirical models based on quantum mechanics to simulate these complex geochemical processes on the atomic scale.

Experimental measurements of the electronic properties of calcite are made more complex by surface charging and decomposition problems. Those spectral measurements that do exist have mostly been determined with X-ray photoemission spectroscopy (XPS) and have concentrated on the core-level photopeaks (Hochella, 1988; Stipp and Hochella, 1991; Baer et al., 1991; Baer et al., 1992). Only recently have detailed lower binding-energy X-ray-generated valence-region photospectra been collected (Baer and Moulder, 1993). He(I), He(II) (Connor et al., 1978), and X-ray photoemission spectra (Calabrese and Hayes, 1975) of weakly bound carbonate salts (K_2CO_3 and Li_2CO_3) have given additional valence information on the carbonate anion. Anisotropic X-ray emission has allowed the σ and π valence electron spectral contributions of the carbonate group to be separated in calcite (Tegeler et al., 1980). X-ray diffraction electron charge-density studies of calcite (Peterson et al., 1979) have shown

* Present address: Complex Systems Theory Branch Code 6690, Naval Research Laboratory, Washington, DC 20375-5000, U.S.A.

0003–004X/94/0304–0205$02.00

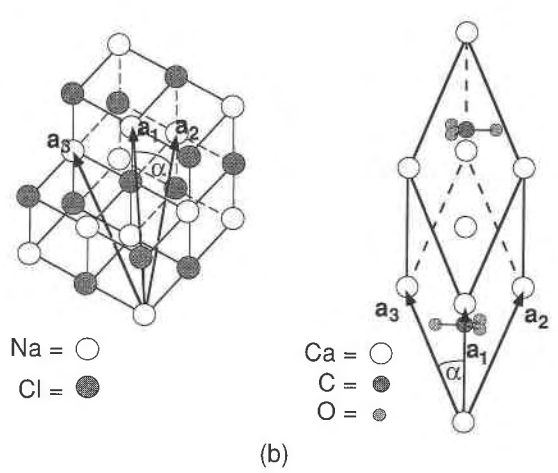

Fig. 1. Comparison of (**a**) the NaCl rock salt unit cell with (**b**) the calcite rhombohedral unit cell.

that charge builds up between the C and O, indicating the covalent nature of the bond. However, because of the difficulty of deconvoluting the thermal motion of the carbonate group, no detailed charge density plots for calcite exist in the literature (Gibbs, personal communication).

Theoretical quantum-mechanical calculations of the electronic and structural properties of calcite are scarce. All have been within a Hartree-Fock formalism and have been used only to calculate effective point charges as input to electrostatic models (Ladd, 1972; Yuen et al., 1978) or to estimate energy differences between various $CaCO_3$ polymorphs (Yuen et al., 1978). These calculations have been limited by the use of finite clusters and small Gaussian basis sets. More recently, good values of the refractive indices of calcite were calculated working within a random phase approximation method and using large Gaussian basis sets (Tossell and Lazzeretti, 1988). However, these calculations must be considered preliminary, as calcite was only modeled by a collection of independent Ca^{2+} and CO_3^{2-} ions. The only other related quantum-mechanical calculations have been on the CO_3^{2-} anion, either isolated (Connor et al., 1972; Random, 1976; Tossell, 1976; Konovalov and Solomonik, 1983; Tossell, 1985; Hotokka and Pyykkö, 1989) or embedded in a lattice of point charges to mimic the calcite crystal environment (Julg and Létoquart, 1977).

In this paper, we calculate the ground-state electronic and structural properties of bulk calcite using density functional theory (DFT) (Hohenberg and Kohn, 1964; Kohn and Sham, 1965) as implemented within the full-potential, linearized augmented plane wave (FLAPW) method (see Jansen and Freeman, 1984). The only inputs to the calculation are the atomic number and position of the constituent atoms in the periodic rhombohedral unit cell. Our results are checked against experimental results where available. The calculated density of states (DOS), in particular, is directly compared with detailed valence band XPS data for calcite (Baer and Moulder, 1993) and reflection electron energy-loss spectroscopy (REELS) measurement of the band gap (Baer and Blanchard, 1993). These latter two measurements were taken especially for comparison with calculations in this paper and are part of a combined experimental and theoretical effort to study the role of calcite in the transport of contaminants in the environment. Study of the calculated charge density reveals the mixed nature of bonding within calcite and the relative sizes of the constituent atoms. Experimentally the carbonate group can be considered isolated from its crystal environment. For example, C-O bond lengths are almost identical in many carbonates (Zemann, 1981) and only change by a small amount under compression (Ross and Reeder, 1992). Current empirical atomic scale models of carbonates (e.g., Dove et al., 1992) exploit this by treating the carbonate group as a rigid, incompressible unit. In this paper, we further test the environmental independence of the carbonate group by calculating the change in the C-O bond length under compression for calcite.

Bulk structure

The structure of calcite has the space group $R\bar{3}c$ and can be thought of as a distorted rock salt structure. To demonstrate this, we start with the undistorted NaCl rock salt structure given in Figure 1a. For this structure the primitive basis translations are the vectors $\mathbf{a}_1$, $\mathbf{a}_2$, and $\mathbf{a}_3$, where the vectors are of equal length and are at angles of 33.6° to each other. The primitive rhombohedral unit cell of calcite (Fig. 1b) can be obtained by replacing Na atoms with Ca atoms, each Cl atom with the C atom at the center of each carbonate group, and uniformly compressing this structure along the threefold symmetry axis [111] so that the translational vectors make angles of approximately 46° with one another.

The primitive rhombohedral unit cell of calcite contains ten atoms (two $CaCO_3$ formula units) and consists of alternating (111) planes of Ca atoms and carbonate groups. Ca atoms are situated at 0 and ½ along [111], and carbonate groups are located at ¼ and ¾ along this vector. Each carbonate group forms an equilateral triangle lying in the (111) plane, and carbonate groups in adjacent carbonate layers are rotated by 60° with respect to one another. Three structural parameters are needed to describe the calcite structure: a, the length of each translational vector; α, the angle between them; and u, a parameter proportional to the C-O bond length. In Table 1 we list the experimental equilibrium rhombohedral structural parameters for calcite (Reeder, 1983), together with the equilibrium C-O bond length d(C-O) and the primitive unit-cell volume V_0. These values were determined from the alternative hexagonal lattice description of calcite (p. 8, Reeder, 1983). To denote the calcite cleavage plane, instead of using the rhombohedral indices (211) we use the hexagonal indices $(10\bar{1}4)$, as that has become the standard notation quoted in the literature.

Density functional theory within the local density approximation

General method

To calculate the zero-temperature ground-state properties of bulk calcite, we use density functional theory (DFT) (Hohenberg and Kohn, 1964; Kohn and Sham, 1965), modeling exchange-correlation effects within the local-density approximation (LDA) (Hedin and Lundqvist, 1971). As a first principle, or ab initio, method, the only inputs to a static calculation at a fixed geometry are the position and atomic number of each atom in the unit cell. Within the DFT-LDA method there are no restrictions on the types of atom, bonding, or material that can be considered. For mixed bonding systems, such as calcite, that is essential, as the ionic and covalent bonding must be treated on equal terms. Working within the LDA, ground-state properties and valence band spectra are well produced. Structural parameters and elastic moduli typically can be computed to within 5 and 20% of the corresponding experiment values. For an excellent review of density functional theory, consult the paper by Jones and Gunnarsson (1989).

Within the DFT formalism, the total energy of a many electron system can be written exactly as a functional of the electron charge density, ρ (Hohenberg and Kohn, 1964). To calculate the ground-state electron density, and hence the ground-state total energy, of a particular system, a series of coupled eigenvalue equations (Kohn and Sham, 1965),

$$(-\nabla^2 + V_{\text{eff}}[\rho])\psi_n = E_n\psi_n \quad (1)$$

need to be solved. For these one electron equations, each electron moves in an effective potential, $V_{\text{eff}}[\rho]$, that describes its interaction with the fixed atomic nuclei and all the other remaining electrons. The charge density,

$$\rho = \sum_{n,\text{occupied}} |\psi_n|^2 \quad (2)$$

can then be constructed from the eigenfunctions, ψ_n, by summing over all occupied states. Because the effective potential, $V_{\text{eff}}[\rho]$, depends explicitly on the charge density, ρ, Equations 1 and 2 must be solved self-consistently.

To solve these one electron equations, we use the FLAPW method (see Jansen and Freeman, 1984). This is the most precise implementation of DFT. No shape approximations are made for the potential $V_{\text{eff}}[\rho]$, and all core and valence electrons are treated explicitly. Each one electron equation is solved using a linearized, augmented plane wave (LAPW) basis (Andersen, 1973; Koelling and Arbman, 1975). These LAPW basis functions are defined as follows. In spherical regions centered about each atom, atomic basis functions are used, whereas in the remaining interstitial region, a plane wave is used. The solutions are then matched at the boundary, and the energy dependence, which is inherent in the traditional augmented plane wave (APW) method (Loucks, 1967), is removed by linearizing about a typical energy for the band of interest.

Table 1. Comparison of calculated equilibrium lattice parameters, C-O bond length, unit-cell volume, and bulk modulus with experimental values

	Theory (this study)	Experiment
a (Å)	6.201	6.375*
α (°)	48.3	46.1*
u	0.2651	0.2568*
d(C-O) (Å)	1.346	1.281*
V_0 (Å^3)	121.96	122.62*
K_0 (GPa)	57	71.07**, 71.56†, 73.15‡

* Derived from hexagonal description of calcite (see Reeder, 1983).
** Measurements were taken at 298 K for a single calcite crystal (Singh and Kennedy, 1974).
† Kaga (1968).
‡ Bridgman (1925).

Within the FLAPW method, the numerical error in the total energy scales with the number of basis functions used (Jansen and Freeman, 1984). The total energy for an infinite basis can then be extrapolated from finite size basis results. The FLAPW method thus allows energy differences between distorted geometries or different polytopes to be calculated precisely. Realistic estimates of absolute and relative errors in the total energies can also be obtained. This implementation of density-functional theory has been used to study metals (Jansen and Freeman, 1984), semiconductors (Massidda et al., 1990), ionic solids (Jansen and Freeman, 1986), and molecular solids (Min et al., 1986). Recent applications of this method include calculating the Fermi surface for new cuprate high-temperature superconductors (Pickett et al., 1992) and the elastic moduli of Al-rich Al-Li compounds (Mehl, 1993). Equations of state and electronic properties of minerals such as $MgSiO_3$ perovskite (Cohen, 1989), stishovite SiO_2 (Cohen, 1991), and CaO and MgO (Mehl et al., 1988) have also been studied. This applicability to such a wide range of materials, together with the ability to obtain realistic estimates of errors incurred, gives us confidence that this method is appropriate for the study of calcite.

Although the FLAPW method is a numerically precise method for solving the DFT-LDA equations and calculating total energies, it is also one of the more computationally intensive. The exact central processing unit (cpu) time depends on the type and number of atoms in the unit cell, the number of basis functions, and the number of integration **k** points used. For calcite, with ten atoms in the unit cell, a large basis of 126 functions per atom, and 20 integration **k** points, each bulk total energy calculation takes approximately 13 cpu h per geometry on a Cray Y-MP.

Details of calcite calculation

For the FLAPW calculations described in this work for bulk calcite, the C and O 2s and 2p orbitals along with the Ca 3p and 4s orbitals are treated as valence states. All the remaining electrons are defined to be core electrons. For the valence electrons, one electron eigenvalues are calculated within a semirelativistic approximation

Table 2. Comparison of the calculated bonded radii with ionic and covalent radii for Ca, C, and O atoms

Atom	Bonded radius (Å)	Ionic radius* (Å)	Covalent radius* (Å)
Ca	1.18**	0.99	—
C	0.40†	0.15	0.77
O	1.18** 0.88†	1.40	0.66

* Kittel (1986).
** Calculated from the Ca-O bond.
† Calculated from the C-O bond.

(MacDonald et al., 1980) and using a single energy window, whereas for core electrons the one electron eigenvalues are treated fully relativistically. Janak's (1978) parameterized form of the local density approximation is used throughout. A periodic primitive rhombohedral unit cell (Fig. 1b) for calcite is used for all our calculations (no finite cluster approximations were made to simulate the bulk system). Atomic units of energy, the Rydberg (Ry), and of distance, the Bohr, are used (1 Ry = 13.6058 eV and 1 Bohr = 0.529 Å). However, in Tables 1 and 2 distances are given in ångströms.

The principal numerical convergence parameters within the FLAPW calculation are the number of **k** points used to perform Brillouin zone integrations and the number of augmented plane waves used to expand the one electron eigenfunctions in Equation 1. After extensive convergence tests, 20 **k** points and over 126 basis functions per atom (a cutoff of $k_{max} = 4.5$) were used for the electronic structure and charge-density calculations reported here. This yields relative errors in the total energy differences of <2 mRy per atom. To calculate the equilibrium geometry and bulk modulus, we used a smaller basis set on the order of 60 basis functions per atom ($k_{max} = 3.5$), together with 10 **k** points. In this case, relative errors were larger, on the order of 5 mRy per atom. The details of the convergence test and values of various series cutoffs used in this calculation are given in the appendix.

Results

Structural parameters

To determine the equilibrium structure and bulk modulus for calcite as predicted within the DFT-LDA method, we calculated the total energy of bulk calcite at 0.9, 1.0, and 1.1 of the observed experimental equilibrium volume V_0. At each volume, the energy was calculated for three values of the angle α and for three C-O bond lengths. In total, the energies of 27 distorted calcite structures were determined. A quadratic fit was then used to determine the optimal angle and C-O distance that minimized the energy at each volume. To calculate the energy at each geometry, a basis set of about 60 functions per atom ($k_{max} = 3.5$) was used, and integration was performed with 10 **k** points. A basis set of this size must be considered small for these types of calculation, and, although structural properties are well produced, properties

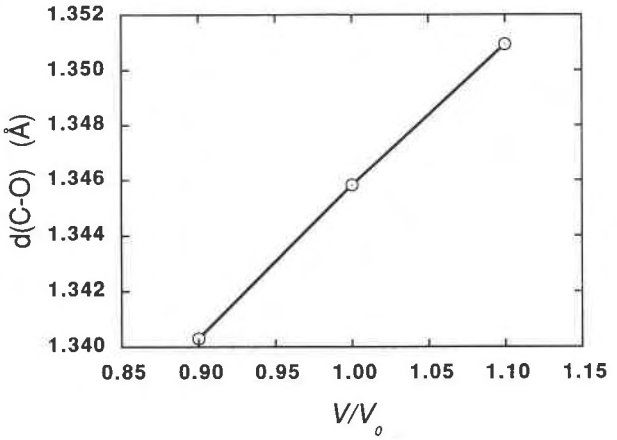

Fig. 2. Calculated change in the C-O bond length with volume.

that depend on the accurate determination of energy difference are less accurate. Our calculation of the bulk modulus to follow must therefore must be considered as a first estimate.

In Figure 2 the calculated change in the C-O bond length as a function of volume is plotted. Under compression the C-O bond length decreases. For a 5% decrease in volume, we calculated this change to be small, approximately 3 mÅ (or 0.2%). This result compares well with recent structural refinements determined from high-pressure X-ray intensity data for the rhombohedral carbonates dolomite and ankerite (Ross and Reeder, 1992). In that study, a 4% decrease in volume reduced the C-O bond length by 5 ± 3 mÅ. Over this volume range the carbonate group in calcite acts as an incompressible structural unit. Treating the carbonate group as a rigid object within empirical models of calcite (e.g., Dove et al., 1992; Skinner and LaFemina, in preparation) therefore is a good approximation.

The calculated equilibrium structural parameters, C-O bond length, unit-cell volume, and isothermal bulk modulus (K_0) are given in Table 1 as determined from a quadratic fit. Structural parameters are reproduced to within 5% of their experimental values, as given by the recent structural refinement in Reeder (1983). The error in the bulk modulus, as calculated at the predicted LDA volume, is approximately 20% larger. Thermal corrections to our zero temperature calculation would only increase the bulk modulus by approximately 2 GPa, giving a 17% error. The major numerical causes of the error in the calculated bulk modulus are due to the small basis set being used, for which the relative error in the total energy is 5 mRy per atom, and the small number of volume data points that were used. More extensive calculations at a larger number of volume points, using a larger basis set, on the order of 120 functions per atom ($k_{max} = 4.5$), and 20 integration **k** points, would reduce this error. Further improvements may also be obtained if the calculations were restricted to a smaller volume regime. That would allow direct comparison with the experimental measure-

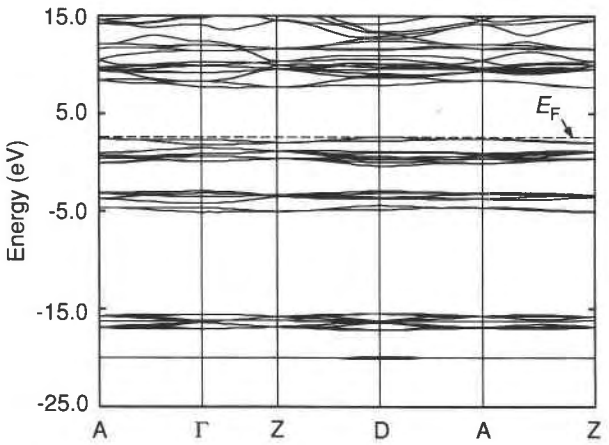

Fig. 3. Electronic band structure for calcite along selected high-symmetry directions as defined by the points **A** (0.5, 0.0, 0.0), Γ (0.0, 0.0, 0.0), **Z** (0.5, 0.5, 0.5), and **D** (0.5, 0.5, 0.0) in the first Brillouin zone (see Fig. 16b of Koster, 1957), where fractional coordinates in parentheses refer to reciprocal lattice vectors. The Fermi energy (E_F) is defined to be at the valence band maximum.

ment of the bulk modulus that uses data only over a 1.6% volume compression regime (Singh and Kennedy, 1974) before calcite transforms to the monoclinic $CaCO_3$-II phase (Merrill and Bassett, 1975). However, to do this, energy differences on the order of 2 mRy must be calculated very accurately. That would require very large basis sets, which are currently computationally prohibitive.

Electronic structure

To calculate the electronic band structure (and the charge density), we worked at the experimental equilibrium geometry for calcite (Reeder, 1983), solving the one electron equation (Eq. 1) with a basis set of over 120 basis functions per atom and 20 integration **k** points. Figure 3 shows the resultant band structure of calcite for selected high-symmetry lines in the first Brillouin zone. The bands are flat, with the highest occupied band completely filled and the lowest unoccupied band completely empty (consistent with calcite being an insulator). The smallest band gap is calculated to be indirect from **D** → **Z**, with a value of 4.4 ± 0.2 eV as extrapolated from careful finite size basis set studies. The experimental value of the band gap is 6.0 ± 0.35 eV (Baer and Blanchard, 1993), as measured by reflection electron energy-loss spectroscopy (REELS). Our calculated value of the band gap is consistent with other DFT calculations, which show that the local density approximation typically underestimates the experimental band gap in solids. The relatively large 27% error in the calculated band gap compared with experiment is also expected, as errors can range from 25 to 80% or more (Pickett, 1986). An improved description of the exchange-correlation effects, beyond the local density approximation, can partially correct for this (Jones and Gunnarsson, 1989).

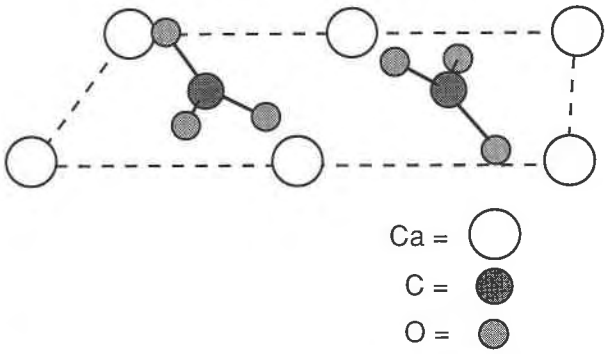

Fig. 4. The relative arrangement of atoms within the calcite $(10\bar{1}4)$ cleavage plane (dashed line).

In the range of energy shown in Figure 3, four occupied bands of well-defined symmetry exist below the Fermi energy (E_F), defined as the valence band maximum. Lowest in energy, at approximately −20 eV, is an atomiclike band of predominantly O 2s character. The next highest band, at −17 to −16 eV, comprised the Ca 3p states, which are raised in energy relative to their atomic levels and mix appreciably with O 2s states in the carbonate group. The broad band at −4 eV is composed of hybridized O 2s, O 2p, C 2s, and C 2p states and represents the bonding states within the carbonate group. Last, the band immediately below the Fermi energy is essentially pure O 2p in character, except for a slight mixing of Ca 4p and 3d states. A detailed discussion of the symmetry character of these bands is given in the next section, along with a discussion of the charge density and the component eigenfunction contour plots.

Charge density and the density of states

X-ray diffraction studies for calcite (Peterson et al., 1979) showed a buildup of charge between the C and O atoms in the carbonate group, indicating its covalent nature. Studies on the rhombohedral carbonate dolomite (Effenberger et al., 1983) showed a similar buildup of charge in the C-O bond and also observed a buildup of charge in the O lone pair regions. However, attempts at producing detailed X-ray diffraction charge-density distributions for calcite have been unsuccessful (Peterson et al., 1979). This is primarily due to the problem of deconvoluting the translational, librational, and (large) screw motion of the carbonate group (Gibbs, personal communication).

In Figure 4 we show the arrangement of atoms in the unrelaxed calcite $(10\bar{1}4)$ cleavage plane (dashed line). For each carbonate group, one C-O bond lies within the plane, whereas the remaining two O atoms lie equidistant above and below the plane, respectively. All Ca atoms lie in the plane. In Figure 5, the calculated bulk charge density within the calcite cleavage plane is given. From this plot the mixed nature of bonding in calcite can be clearly seen. To obtain a quantitative measure of this bonding, the value of the charge density is determined at the points P,

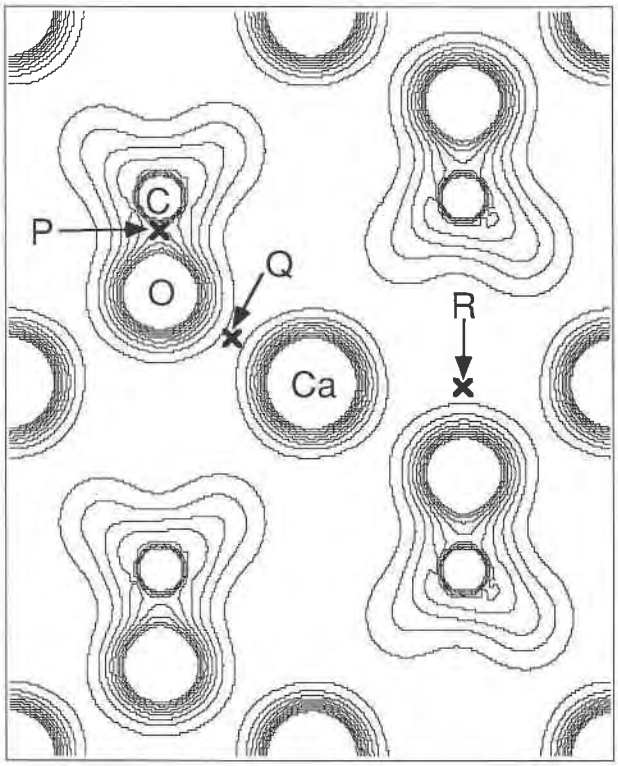

Fig. 5. Charge density for bulk calcite within the $(10\bar{1}4)$ cleavage plane. Two unit cells are shown. Contours are spaced at 0.05 Bohr^{-3} and are in the range 0.05–0.5 Bohr^{-3}.

Q, and R, the midpoints between C-O, Ca-O, and Ca-Ca atoms, respectively. For these points the charge density has the value 0.3, 0.04, and 0.02 Bohr^{-3}, respectively. For an ionic solid such as NaCl, the charge density at the midpoint of the Na-Cl bond is on the order of 0.01 Bohr^{-3}. Comparing our results for calcite with this ionic reference, the C and O atoms are covalently bonded within the carbonate anion, whereas the carbonate group is ionically bonded to the Ca cation. This buildup of charge in the C-O bond is also borne out by calculations on the isolated CO_3^{2-} anion (Tossell, 1985).

Our calculations thus confirm the mixed ionic and covalent bonding within calcite that has been commonly assumed within the mineralogy community. To model accurately the bonding in calcite, it is crucial that the covalent bonding within the carbonate group be included. Point charge models have tried to mimic this covalent bonding by representing the carbonate group charge distribution by a collection of point charges (Ladd, 1972; Yuen et al., 1978). More recently, empirical models for calcite (Dove et al., 1992) have included this covalent character with bond-bending terms. We believe, however, that semiempirical models based on quantum mechanics need to be developed for calcite that explicitly include the covalent nature of bonding within the carbonate group. That would be especially important when simulating processes where electronic effects are expected to be crucial, for example, the substitutional adsorption of Mn cations on the calcite surface (Baer et al., 1991).

Table 3. Net no. of valence electrons within spheres centered on the atoms and in the remaining interstitial (I) region

	No. of electrons		Sphere radius	
	Atom densities*	Bulk calcite**	Bohr	Å
Ca	12.170†	12.653†	2.5	1.323
C	0.512	0.523	0.7	0.370
O	26.346	30.044	1.5	0.794
I	20.972	16.780		
Total	60.000	60.000		

* Distribution obtained from an overlapping of atomic densities placed at the atomic sites.
** Distribution for bulk calcite.
† Ca 3p electrons are treated as valence electrons and included in this sum.

An estimate of the sizes of the atoms in calcite can also be obtained from the charge-density plots in Figure 5, by calculating appropriate bonded radii (Gibbs et al., 1992, and references therein). These bonded radii are defined as the distance along an atomic bond from the point of minimum electron density to the atom centers. For calcite, the bonded radii along the C-O bond within the carbonate group are r(C) = 0.40 and r(O) = 0.88 Å, whereas along the bond formed between each Ca atom and the nearest O atom the bonded radii are r(Ca) = 1.18 and r(O) = 1.18 Å. In Table 2 these values are compared with the standard ionic and covalent radii for these atoms. From these values, it is seen that the radii of the C and O atoms in calcite fall between these two limits. The O anions are 16–37% smaller than those expected based purely upon an ionic picture of atomic size, whereas the Ca cations are 20% bigger. At the calcite cleavage surface, the sizes of these ions control the approach of solvated contaminant ions and the loss of their waters of solvation. If the bonded radius of O determined from the Ca-O bond of 1.18 Å is taken as the measure of the size of an O ion at a calcite surface, then the O anion is the same size as the Ca cation. The comparable size of these ions could therefore have significant consequences for the chemical reactivity of the calcite surface.

Table 3 gives the net number of valence electrons within spheres centered on the atoms and in the interstitial (I) region for bulk calcite. These are compared with the number of valence electrons obtained within these same regions from overlapping Ca, C, and O atomic densities placed at the atomic sites. As with all population analyses, there is no quantitative significance associated with the values of these numbers, since they depend on details of the procedure used to obtain them (in our case the choice of sphere radii). However, a qualitative understanding of how charge is rearranged in the unit cell can be obtained. From Table 3, it is clear that the major redistribution of charge is from the interstitial region to inside the O spheres. This results in a net increase of charge within each O sphere of approximately 0.62 electrons, compared with the neutral atom case. For Ca, there

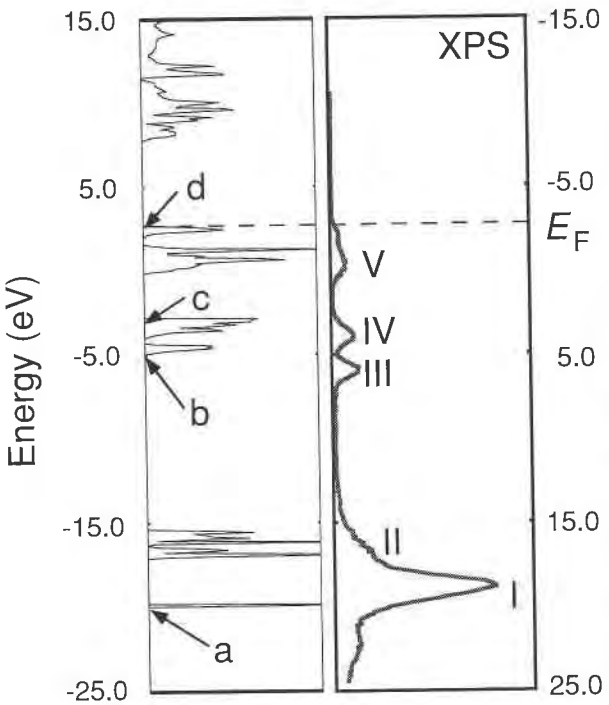

Fig. 6. Comparison of the calculated density of states (**left**) with experimental X-ray photoemission spectrum (XPS) (**right**). To compare bands, the XPS zero of energy has been shifted by 5.5 eV to align the theoretical and experimental valence band maxima. Letters a–d denote the position of the energy eigenvalues corresponding to the eigenfunction components plotted in Fig. 7.

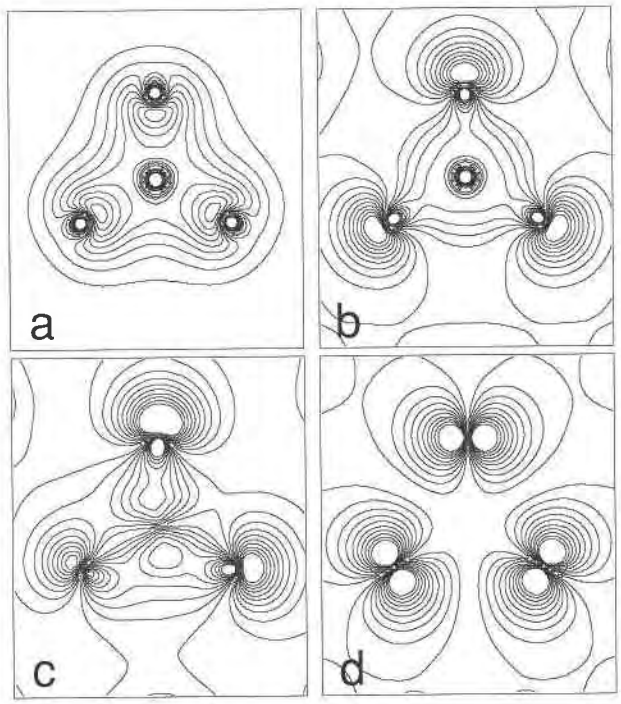

Fig. 7. Real-space contour plots within the (111) carbonate plane of four (**a–d**) eigenfunction components $|\psi_n(\mathbf{r})|^2$ of the charge density, as calculated at $\Gamma(\mathbf{k} = 0)$. In each panel a single carbonate group is shown consisting of three O atoms positioned at the corners of an equilateral triangle and one C atom at the center of the triangle. Contours are spaced at 0.02 $Bohr^{-3}$ and are in the range 0.02–0.2 $Bohr^{-3}$.

is also a net increase in charge of about 0.24 electrons per atom. That conflicts with the classical ionic picture, used in most electrostatic models, of Ca being a divalent cation (Yuen et al., 1978; Singh et al., 1987; Dove et al., 1992). In fact, the atomic Ca 4s orbital is long-range, extending to about 4.0 Bohr (2.116 Å), so that 96% of the Ca 4s electronic charge is within the interstitial region. For the C atom, there is a net increase in charge within the C sphere of 0.006 electron per atom. This change is two orders of magnitude smaller than both the Ca and O cases and is not significant within this simple analysis. In contrast, most single-point ion representations of the carbonate group, obtained through either fitting charge parameters in electrostatic models (Yuen et al., 1978; Singh et al., 1987; Dove et al., 1992) or by Mulliken population analysis in ab initio SCF-MO calculations (Yuen et al., 1978; Connor et al., 1972), find a positive charge on the C atom of approximately +1. The difference between these two analyses is, in part, simply a matter of perspective. In our calculation, the small C sphere radius of 0.7 Bohr (0.370 Å) focuses the analysis near the C atom, where a negligible change of charge occurs. On the other hand, within the single-point ion descriptions of the carbonate group, negative charge is constrained to cling to the atomic sites, as opposed to between the C and O atoms.

From Equation 2 it can be seen that the charge density ρ can be decomposed into the occupied eigenfunction components $|\psi_n(\mathbf{r})|^2$. Although the eigenfunctions $\psi_n(\mathbf{r})$ have no formal physical significance within DFT, they do reveal the symmetry of various states as a function of energy and yield a qualitative insight into the orbital character of the electronic band structure and density of states shown in Figures 3 and 6. To obtain a more detailed understanding of the covalent bonding within the carbonate group, in Figure 7 contour plots of $|\psi_n(\mathbf{r})|^2$, as calculated at Γ ($\mathbf{k} = 0$), are given as a function of position $\mathbf{r}$. Each panel (a–d) shows a single carbonate group within the (111) carbonate plane. The positions of the associated one-electron energy eigenvalues E_n are marked (a–d) on the density of states (DOS) in Figure 6.

For the lowest energy eigenvalue at *a*, a symmetric bonding combination of mainly O 2s (48%) and the C 2s and 2p states in the interstitial region is formed. A small contribution (10%) of O 2p is also present. This results in charge piling up between the C and O atoms in a covalent manner. In contrast, for the eigenvalue at *b*, a symmetric nonbonding combination of mainly O 2p (36%) and O 2s (20%) with C 2s and 2p states is obtained. At that value, charge builds up outside the C-O bond, resulting in orbital lobes on the O atoms pointing away from the central C atom. These lobes are consistent with the observed X-ray diffraction electron-density maxima

in the O lone pair region for the rhombohedral carbonate dolomite (Effenberger et al., 1983). At *c*, a degenerate state, hybrid orbitals are formed between O 2p (49%) and C states, with some mixing of O 2s states (12%). Last, for the highest occupied eigenvalue at *d*, which is positioned at the Fermi energy, the states are nonbonding and have nearly pure O 2p (72%) character, except for a slight mixing of Ca 4p states (2%). In our analysis, the percentage breakdown of the wave functions given in brackets should be taken as only a qualitative measure of orbital character, as these values ultimately depend on the choice of sphere radii used to partition space.

In Figure 6, the valence band X-ray photoemission spectrum (XPS) for bulk calcite (Baer and Moulder, 1993) is compared with the calculated density of states. With allowances for finite temperature broadening of the XPS spectrum, the relative band widths and peak positions are well reproduced within our zero-temperature ground-state calculation. An assignment of the orbital character of the experimental XPS peaks can thus be made by direct comparison with the calculated band structure and density of states. The lowest XPS band at a binding energy of approximately 20 eV is mainly of O 2s character (peak I), with some mixing of Ca 3p states (peak II). At approximately 5 eV, peaks III and IV are due to the mixing of C and O 2s and 2p states within the carbonate group, whereas the highest occupied band at about 2 eV (peak V) is almost pure O 2p states. Peak intensities compare poorly with experimental results, as they ultimately depend on scattering effects and the different cross-sectional areas of s and p electrons; these factors are excluded from the ground-state density-functional formalism used in this paper. However, the excellent agreement in peak positions and band widths demonstrates the important role that ab initio calculations can play in interpreting complex experimental data.

These results, together with previously discussed structural calculations, are currently being used to parameterize computationally economical tight-binding models for the study of calcite surfaces and steps (Skinner and LaFemina, in preparation).

Acknowledgments

The authors would like to thank D.R. Baer, R.E. Cohen, D.L. Blanchard, T.J. Godin, M.J. Mehl, D.M. Sherman, and M.F. Stave for enlightening discussions and practical comments during the course of our research and L. Rivenbark for careful proofreading of this manuscript. In addition, we would like to thank D.R. Baer and D.L. Blanchard for allowing us to use their XPS and REELS data for calcite prior to publication. Correspondence with G.V. Gibbs, S.C. Nyberg, and P.S. Yuen concerning their work is also appreciated. J.P.L acknowledges the support of the Geosciences Research Program, Division of Engineering and Geosciences, U.S. Department of Energy, under contract number DE-AC06-76RLO 1830 with Battelle Memorial Institute, which operates the Pacific Northwest Laboratory. For computing facilities we would like to acknowledge the support of the National Energy Research Supercomputing Center.

References cited

Andersen, O.K. (1973) Simple approach to the band-structure problem. Solid State Communications, 13, 133–136.

Baer, D.R., and Blanchard, D.L., Jr. (1993) Studies of the calcite cleavage surface for comparison with calculation. Applied Surface Science, 72, 295–300.

Baer, D.R., and Moulder, J.F. (1993) High resolution XPS spectrum of calcite ($CaCO_3$). Surface Science Spectra, 2, 1–7.

Baer, D.R., Blanchard, D.L., Engelhard, M.H., and Zachara, J.M. (1991) The interaction of water and Mn with surfaces of $CaCO_3$: An XPS study. Surface and Interface Analysis, 17, 25–30.

Baer, D.R., Marmorstein, A.M., Williford, R.E., and Blanchard, D.L. (1992) Comparison spectra for calcite by XPS. Surface Science Spectra, 1, 80–86.

Bridgman, P.W. (1925) Linear compressibility of fourteen natural crystals. American Journal of Science, 210, 483–498.

Calabrese, A., and Hayes, R.G. (1975) Valence level studies of some first and second row oxyanions by x-ray photoelectron spectroscopy. Journal of Electron Spectroscopy and Related Phenomena, 6, 1–16.

Cohen, R.E. (1989) Electronic structure calculations for oxide perovskites and superconductors. In A. Navrotsky and D.J. Weidner, Eds., Perovskite: A structure of great interest to geophysics and mineral science, p. 55–66. American Geophysical Union, Washington, DC.

——— (1991) Bonding and elasticity of stishovite SiO_2 at high pressure: Linearized augmented plane wave calculation. American Mineralogist, 76, 733–742.

Connor, J.A., Hillier, I.H., Saunders, V.R., and Barber, M. (1972) On the bonding of the ions PO_4^{3-}, SO_4^{2-}, ClO_3^- and CO_3^{2-} as studied by x-ray spectroscopy and ab initio SCF-MO calculations. Molecular Physics, 23, 81–90.

Connor, J.A., Considine, M., and Hillier, I.H. (1978) Low energy photoelectron spectroscopy of solids. Chemical Society Journal: Faraday Transactions II, 74, 1285–1291.

Davis, J.A., Fuller, C.C., and Cook, D. (1987) A model for trace metal sorption processes at the calcite surface: Adsorption of Cd^{2+} and subsequent solid solution formation. Geochimica et Cosmochimica Acta, 51, 1477–1490.

Dove, M.T., Winkler, B., Leslie, M., Harris, M.J., and Salje, E.K.H. (1992) A new interatomic potential model for calcite: Applications to lattice dynamics studies, phase transitions, and isotope fractionation. American Mineralogist, 77, 244–250.

Effenberger, H., Kirfel, A., and Will, G. (1983) Studies on the electron density distribution of dolomite $CaMg(CO_3)_2$. Tschermaks mineralogische-petrographische Mitteilungen, 31, 151–164 (in German).

Gibbs, G.V., Spackman, M.A., and Boisen, M.B. (1992) Bonded and promolecule radii for molecules and crystals. American Mineralogist, 77, 741–750.

Hedin, L., and Lundqvist, B.I. (1971) Explicit local exchange-correlation potentials. Journal of Physics C, 4, 2064–2083.

Hirano, S., Yogo, T., and Kikuta, K. (1991) Synthetic calcite single crystals for optical device. Progress in Crystal Growth and Characterization of Materials, 23, 341–367.

Hochella, M.F. (1988) Auger electron and x-ray photoelectron spectroscopies. In Mineralogical Society of America Reviews in Mineralogy, 18, 573–637.

Hochella, M.F., and White, A.F. (1990) Mineral-water interface geochemistry: An overview. In Mineralogical Society of America Reviews in Mineralogy, 23, 1–16.

Hohenberg, P., and Kohn, W. (1964) Inhomogeneous electron gas. Physical Review, 136, 864–871.

Hotokka, M., and Pyykkö, P. (1989) An ab initio study of bonding trends in the series BO_3^{3-}, CO_3^{2-}, NO_3^- and $O_4(D_{3h})$. Chemical Physical Letters, 157, 415–418.

Janak, J.F. (1978) Itinerant ferromagnetism in fcc cobalt. Solid State Communications, 25, 53–55.

Jansen, H.J.F., and Freeman, A.J. (1984) Total-energy, full-potential linearized augmented plane-wave method for bulk solids: Electronic and structural properties of tungsten. Physical Review B, 30, 561–569.

——— (1986) Structural properties and electron density of NaCl. Physical Review B, 33, 8629–8631.

Jones, R.O., and Gunnarsson, O. (1989) The density functional formalism, its applications and prospects. Review in Modern Physics, 61, 689–746.

Julg, A., and Létoquart, D. (1977) Modifications of certain properties of

carbonate and nitrate ions due to the influence of the crystalline environment. Nouveau Journal de Chimie, 1, 261–263.
Kaga, H. (1968) Third-order elastic constants of calcite. Physical Review, 172, 900–919.
Kittel, C. (1986) Introduction to solid state physics (6th edition), p. 76. Wiley, New York.
Koelling, D.D., and Arbman, G.O. (1975) Use of energy derivative of the radial solution in an augmented plane wave method: Application to copper. Journal of Physics F, 5, 2041–2053.
Kohn, W., and Sham, L.J. (1965) Self-consistent equations including exchange and correlation effects. Physical Review, 140, A1133–1138.
Konovalov, S.P., and Solomonik, V.G. (1983) Theoretical study of the electronic and geometric structure, force fields, and vibrational spectra of free BO_2^-, NO_3^- and CO_3^{2-} ions. Russian Journal of Physical Chemistry, 57, 384–386.
Koster, G.F. (1957) Space groups and their representations. In F. Seitz and D. Turnball, Eds., Solid State Physics (vol. 5), p. 194–211. Academic, New York.
Ladd, M.F.C. (1972) Charge distributions through energetics. Nature Physical Sciences, 238, 125–126.
Loucks, T.L. (1967) Augmented plane wave method, 256 p. W.A. Benjamin, New York.
MacDonald, A.H., Pickett, W.E., and Koelling, D.D. (1980) A linearised relativistic augmented-plane-wave method utilising approximate pure spin basis functions. Journal of Physics C, 13, 2675–2683.
Massidda, S., Continenza, A., Freeman, A.J., dePascale, T.M., Meloni, F., and Serra, M. (1990) Structural and electronic properties of narrow-band-gap semiconductors: InP, InAs and InSb. Physical Review B, 41, 12079–12085.
Mehl, M.J. (1993) Pressure dependence of the elastic moduli in aluminum-rich Al-Li compounds. Physical Review B, 47, 2493–2500.
Mehl, M.J., Cohen, R.E., and Krakauer, H. (1988) Linearized augmented plane wave electronic structure calculations of MgO and CaO. Journal of Geophysical Research, 93, 8009–8022; 94, 1977.
Merrill, L., and Bassett, W.A. (1975) The crystal structure of $CaCO_3$(II), a high pressure metastable phase of calcium carbonate. Acta Crystallographica, B31, 343–349.
Min, B.I., Jansen, H.J.F., and Freeman, A.J. (1986) Pressure induced electronic and structural phase transitions in solid hydrogen. Physical Review B, 33, 6383–6390.
Peterson, R.G., Ross, F.K., Gibbs, G.V., Chiari, G., Gupta, A., and Tossell, J.A. (1979) Electron density study of calcite (abs.). Eos, 60, 415.
Pickett, W.E. (1986) Density functionals in solids II: Excitations. Comments on Solid State Physics, 12, 57–68.
Pickett, W.E., Krakauer, H., Cohen, R.E., and Singh, D.J. (1992) Fermi surfaces, Fermi liquids and high temperature superconductors. Science, 255, 46–54.
Random, L. (1976) Structures of the simple anions from ab initio molecular orbital calculations. Australian Journal of Chemistry, 29, 1635–1640.
Reeder, R.J. (1983) Crystal chemistry of the rhombohedral carbonates. In Mineralogical Society of America Reviews in Mineralogy, 11, 1–47.
Ross, N.L., and Reeder, R.J. (1992) High-pressure structural study of dolomite and ankerite. American Mineralogist, 77, 412–421.
Schmalz, R.F. (1972) Calcium carbonate: Geochemistry. In R.W. Fairbridge, Ed., The encyclopedia of geochemistry and environmental sciences, p. 104–117. Van Nostrand Reinhold, New York.
Singh, A.K., and Kennedy, G.C. (1974) Compression of calcite to 40kbar. Journal of Geophysical Research, 79, 2615–2622.
Singh, R.K., Gaur, N.K., and Chaplot, S.L. (1987) Lattice dynamics of molecular calcite crystals. Physical Review B, 35, 4462–4471.
Stipp, S.L., and Hochella, M.F., Jr. (1991) Structure and bonding environments at the calcite surface as observed with X-ray photoelectron spectroscopy (XPS) and low energy electron diffraction (LEED). Geochimica et Cosmochimica Acta, 55, 1723–1736.
Tegeler, E., Kosuch, N., Wiech, G., and Faessler, A. (1980) Molecular orbital analysis of the CO_3^{2-} ion by studies of the anisotropic x-ray emission of its components. Journal of Electron Spectroscopy and Related Phenomena, 18, 23–28.
Tossell, J.A. (1976) SCF-$X\alpha$ studies of the electronic structures of C, Si and Ge oxides. Journal of Physics and Chemistry of Solids, 37, 1043–1050.
——— (1985) Ab initio SCF MO and modified electron gas studies of electron deficient anions and ion pairs in mineral structures. Physica, 131B, 283–289.
Tossell, J.A., and Lazzeretti, P. (1988) Ab initio calculation of the refractive indices and related properties of $CaCO_3$. Physical Review B, 38, 5694–5698.
Winchester, J.W. (1972) Buffer system. In R.W. Fairbridge, Ed., The encyclopedia of geochemistry and environmental sciences, p. 95–98. Van Nostrand Reinhold, New York.
Yuen, P.S., Lister, M.W., and Nyburg, S.C. (1978) The four-center charge distribution of the carbonate ion and the lattice energies of calcite and aragonite. Journal of Chemical Physics, 68, 1936–1941.
Zachara, J.M., Cowan, C.E., and Resch, C.T. (1991) Sorption of divalent metals on calcite. Geochimica et Cosmochimica Acta, 55, 1549–1562.
Zemann, J. (1981) Zur Stereochemie der Karbonate. Fortschritte der Mineralogie, 59, 95–116.

Manuscript received May 7, 1993
Manuscript accepted November 19, 1993

Appendix 1. Numerical convergence tests

In this appendix, we present the numerical details of the calculations and discuss the convergence of the total energy with the number of **k** points and basis functions.

At each calcite geometry, nonoverlapping spheres of radii 2.5 Bohr (1.323 Å), 0.7 Bohr (0.370 Å), and 1.5 Bohr (0.794 Å) centered on the Ca, C, and O atoms, respectively, were chosen to divide up space. The radius of the C sphere was smaller than what we would have liked to use. However, our choice was restricted by the small C-O bond length of 1.281 Å. If the spheres were not to overlap for the range of volumes of interest, then the sum of the C and O sphere radii had to be less than this value. Ultimately, the radii of these spheres do not affect the converged value of the energy, but they do control the rate of convergence. The charge density ρ and the one electron potential $V_{\text{eff}}[\rho]$ are then expanded in terms of spherical harmonics Y_{lm} within the spheres and plane waves $e^{i\mathbf{g}\cdot\mathbf{r}}$ in the interstitial region between the spheres. For calcite, we truncated these expansions at $l = 6$ and for all reciprocal lattice vectors **g** such that $|\mathbf{g}| < k_{\text{star}} = 9.0$ au. Higher expansions in l of the potential and density typically change the total energy by <0.5 mRy (Jansen and Freeman, 1984). (If we had used only the $l = 0$ component and a single plane wave at $\mathbf{k} = 0$, that would correspond to a muffin-tin approximation for the potential.)

Each angular momentum component L of the LAPW basis function inside the spheres is characterized by an energy parameter E_L. For calcite, all functions from $L = 0$ through to $L = 10$ were included, giving 33 energy parameters to be determined. For the well-defined Ca 3p, O 2s, and O 2p bands, the corresponding energy parameters, E_p[Ca], E_s[O], and E_p[O], were chosen to be at the center of each band. All other energy parameters were set to the energy O p level, E_p[O], as that is the largest source of electrons. The number of basis functions used in our calculation was controlled by a cutoff parameter k_{max}. For a particular integration point **k**, all basis functions labeled by the reciprocal lattice vector **g** were generated such that $|\mathbf{k} - \mathbf{g}| < k_{\text{max}}$.

To determine the appropriate numbers of **k** points and basis functions to use, extensive convergence tests were performed. For $k_{\text{max}} = 3.5$, the number of **k** points was varied from 10 through 80. For 20 **k** points, the total energy was well converged to within an asymptotic regime, in which the relative errors were <2.0 mRy per atom. To investigate the convergence of the total energy with the number of basis functions, k_{max} was varied from

3.5 (approximately 60 basis functions per atom) to 4.5 (over 120 basis functions per atom). The associated total energies, $E_{tot}(k_{max})$ were then linearly fitted to an equation of the form $E_{tot}(k_{max}) = E_{tot}(\infty) + A/(k_{max})^{4.75}$. Comparison of the finite basis results with the extrapolated total energy $E_{tot}(\infty)$ allowed estimates of the absolute and relative errors in the energy to be obtained. For $k_{max} = 4.5$, although the absolute error in the total energy was large, on the order of 50 mRy per atom, relative errors in the total energy between the experimental geometry and a distorted calcite structure were <2 mRy per atom. [The parameters for the distorted calcite structure were $\alpha = 35°$, volume $= 0.9V_0$, and d(C-O) = 1.281 Å.]

For the calculation of the electronic structure and charge density, 20 **k** points and a cutoff of $k_{max} = 4.5$ were chosen. This choice of parameters resulted in a basis set size of over 120 functions per atom and principal energy parameters of E_p[Ca] = −1.1936, E_s[O] = −1.2224, and E_p[O] = 0.032 Ry at the experimental geometry.